© 2019. Published by The Company of Biologists Ltd | Journal of Cell Science (2019) 132, jcs224055. doi:10.1242/jcs.224055

RESEARCH ARTICLE

Upf1 regulates neurite outgrowth and branching by transcriptional and post-transcriptional modulation of *Arc*

Hye Guk Ryu[1], Ji-Young Seo[2], Youngseob Jung[2], Sung Wook Kim[2], Eunah Kim[1], Sung Key Jang[1] and Kyong-Tai Kim[1,2,*]

ABSTRACT

A large number of neuronal proteins must show correct spatiotemporal localization in order to carry out their critical functions. The mRNA transcript for the somatodendritic protein activity-regulated cytoskeleton-associated protein (Arc; also known as Arg3.1) contains two conserved introns in the 3′ untranslated region (UTR), and was proposed to be a natural target for nonsense-mediated mRNA decay (NMD). However, a well-known NMD component Upf1 has differential roles in transcriptional and translational regulation of *Arc* gene expression. Specifically, Upf1 suppresses *Arc* transcription by enhancing destabilization of mRNAs encoding various transcription factors, including Mef2a. Upf1 also binds to the *Arc* 3′UTR, resulting in suppression of translation. Surprisingly, the *Arc* transcript escapes from Upf1-mediated NMD by binding to Ago2 (also known as miRISC), which blocks NMD and further suppresses *Arc* mRNA translation. Upf1 knockdown triggered sustained Arc expression, which contributes to Cofilin (also known as Cfl1) hyperphosphorylation and abnormal neuronal outgrowth and branching. Collectively, these data reveal that multiple levels of Upf1-mediated inhibition of *Arc* gene expression may allow neurons to more effectively respond to changes in neuronal activity.

KEY WORDS: 3′UTR, Arc, NMD, Upf1, Transcription, Translation

INTRODUCTION

Activity-dependent changes in synaptic strength, as observed in long-term potentiation (LTP) and long-term depression (LTD), are considered to be the leading cellular mechanisms underpinning learning and memory (Bliss and Collingridge, 1993). Neurons can coordinate activity-dependent processes through the activation of new gene transcription, and the protein synthesis underlying that synaptic plasticity is critically controlled at the level of mRNA translation (Klann and Dever, 2004). Alteration in the expression of immediate early genes (IEGs) is the first genetic response to a variety of cellular stimuli (Lanahan and Worley, 1998). The somatodendritic protein activity-regulated cytoskeleton-associated protein (Arc; also known as Arg3.1), is one such IEG, and has been the focus of several studies that have shown it to be involved in activity-dependent synaptic plasticity, including both LTP and LTD (Bramham et al., 2010, 2008; Plath et al., 2006). In *Arc* knockout (KO) mice, early-phase LTP is enhanced, whereas late-phase LTP is blocked, and acute knockdown of Arc also results in LTP disruption (Messaoudi et al., 2007). Furthermore, in hippocampal slices from *Arc* KO mice, mGluR (also known as Grm) protein-dependent LTD is suppressed, and *Arc* KO neurons fail to decrease surface expression of the α-amino-3-hydroxy-5-methyl-4-isoxazolepropionic acid receptor (AMPAR) after dihydroxyphenylglycine application (Park et al., 2008).

A previous study has established a critical role for nonsense-mediated mRNA decay (NMD) in regulation of *Arc* expression, and this suggests that this pathway could function to prevent improper Arc protein synthesis at undesired times and/or locations (Giorgi et al., 2007). Seemingly confirming the functional impact of NMD, knockdown of the exon junction complex (EJC) core protein, eIF4AIII, enhances *Arc* mRNA and protein expression. However, unexpectedly, this knockdown also upregulates AMPAR levels at synapses and selectively increases the amplitude of miniature excitatory postsynaptic currents, even though Arc levels are elevated. It is quite a contradictory response because enhanced levels of Arc trigger reduction of surface AMPAR at synapses. Thus, these data suggest that post-transcriptional regulation by NMD is insufficient to fully explain the role of *Arc* gene regulation in synaptic plasticity, and, therefore, gaining understanding of additional mechanisms for maintaining the tight regulation of *Arc* gene expression will be critical for elucidating the precise role of Arc expression in neuronal cells.

Here, we investigated the role of Upf1, an essential component of the NMD pathway, in *Arc* gene regulation to better understand how NMD regulates *Arc* mRNA stability and expression. Interestingly, we found that Upf1 functions at both the transcriptional and translational level to inhibit *Arc* gene expression. Upf1 suppresses *Arc* transcription by downregulating transcription factors that promote *Arc* expression, including Mef2a. Moreover, we show that Upf1 also binds to the *Arc* 3′ untranslated region (UTR) and suppresses translation. Intriguingly, however, *Arc* mRNA can escape from the NMD pathway through the action of Ago2 (also known as miRISC), which binds to the 3′UTR and further represses *Arc* translation, thus inhibiting NMD. Collectively, these data imply that Upf1 is crucial for maintaining low expression levels of Arc under normal conditions, which likely contribute to rapid and selective Arc induction in response to vigorous neuronal activity.

RESULTS

Upf1 suppresses transcription of *Arc*

A simultaneous analysis of the pre-mRNA and mRNA abundance of selected transcripts found that only a minority of UPF1-dependent genes are directly regulated by this protein (Viegas et al., 2007). Tani et al. (2012) additionally measured the genome-wide steady-state abundance and decay rates of mRNAs using RNA sequencing (RNA-seq) and 5′-bromouridine immunoprecipitation

[1]Department of Life Sciences, Pohang University of Science and Technology (POSTECH), Pohang 37673, Republic of Korea. [2]Division of Integrative Biosciences and Biotechnology, Pohang University of Science and Technology (POSTECH), Pohang 37673, Republic of Korea.

*Author for correspondence (ktk@postech.ac.kr)

S.W.K., 0000-0001-7292-2627; K.-T.K., 0000-0001-7292-2627

Received 16 August 2018; Accepted 16 December 2018

Journal of Cell Science (2019) 132, jcs224055. doi:10.1242/jcs.224055

chase sequencing (BRIC-seq), and identified indirect UPF1 targets with >2-fold upregulation, but unaltered decay rates, in UPF1-depleted HeLa cells. These results suggest that many genes are regulated by UPF1 at the transcriptional level, independent of NMD. Therefore, in order to determine whether *Arc* transcription is similarly regulated by Upf1, we measured steady-state *Arc* mRNA levels, using primer sets specific to the mature and premature transcripts, as illustrated in Fig. 1A. Mouse Neuro-2a (N2a) cells were transfected with a short hairpin RNA (shRNA) that targets Upf1, and we first confirmed that this results in a decreased level of Upf1 protein (Fig. 1B). We then found that levels of both the mature and premature *Arc* mRNA were significantly increased in Upf1 knockdown cells (Fig. 1C,D).

The promoters and enhancers that contribute to activity-dependent *Arc* expression have been well characterized (Kawashima et al., 2009). For example, the rapid transcription of *Arc* as an immediate early gene (IEG) is dependent on a critical synaptic activity-responsive element (SARE), which was identified as a unique, ∼100 bp element, located >5 kb upstream of the *Arc* transcription initiation site in the mouse genome. Here, we generated an *Arc*-luciferase reporter vector containing a SARE sequence fused directly upstream of ArcMin, a TATA-containing sequence near the transcription initiation site of the *Arc* gene (Fig. 1E). This distally located SARE-promoter fusion was found to be sufficient to replicate crucial properties of endogenous *Arc* transcriptional regulation (Fig. 1F). Moreover, to investigate the possibility of transcriptional regulation by Upf1, we then measured *Arc* reporter activity in Upf1 knockdown cells. We found that *Arc* promoter activation was increased in cells with shRNA-mediated Upf1 knockdown, as evidenced by a ∼2-fold increase in luciferase activity (Fig. 1G). Together, these results suggest that Upf1 exerts a negative regulatory effect on *Arc* transcription.

Next, we employed the CRISPR/Cas9 system to develop a method for efficient KO of Upf1. A single-guide RNA (sgRNA) was designed to target the Cas9 endonuclease to sites within exon 1 of the *Upf1* gene (Fig. S1A). We tested several cell lines containing a homozygous deletion in Cas9+our sgRNA, and found two, #3 and #13, with decreased levels of Upf1. Of these, only the #3 line showed complete Upf1 KO with no residual expression, as well as strong induction of Arc protein levels; we therefore used the Cas9 +sgRNA #3 cell line (referred to as KO cells) for all studies past this point (Fig. S1B). We then validated efficient KO of Upf1 using different antibodies (Fig. S1C) and dual-color fluorescent protein-based reporters (Pereverzev et al., 2015) for quantification of NMD activity using fluorescence microscopy (Fig. S2D,E). We also performed a rescue experiment by re-expressing Upf1 in Upf1-depleted cells to ensure proper selection (Fig. S2F). Consistent with our results from experiments employing transient shRNA-mediated Upf1 knockdown, the levels of both mature and premature *Arc* mRNA were found to be significantly increased in Upf1 KO cells (Fig. 2A–D). Also, *Arc* promoter activity was higher in KO cells than in wild-type (WT) cells (Fig. 2E,F).

The transcription factor myocyte enhancer factor 2a (Mef2a) has been found to suppress the number of excitatory synapses via induction of its target genes, *Arc* and synaptic Ras-GTP-activating protein 1 (*SynGAP1*) (Flavell et al., 2006). We therefore investigated the potential role of Upf1 in *Mef2a* mRNA regulation. Our data showed that the level of mature *Mef2a* mRNA was significantly higher in Upf1 KO cells; however, *Mef2a* pre-mRNA levels were unaffected (Fig. 2G,H). Based on these results, we hypothesized that Upf1 regulates *Mef2a* transcript stability. We conducted an *in vitro* binding assay using *in vitro* transcribed, biotin-conjugated *Mef2a* 3′ UTR with N2a cell lysate. Fig. 2I shows that Upf1 binds to *Mef2a* 3′ UTR *in vitro*. To determine whether Upf1 is associated with *Mef2a* mRNA *in vivo*, we performed RNA immunoprecipitation (RNA-IP) followed by quantitative RT-PCR (qRT-PCR). Consistent with our hypothesis, *Mef2a* transcripts were found to be enriched in Upf1-specific RNA immunoprecipitates, compared with IgG controls (Fig. 2J). Moreover, Mef2a protein levels were significantly increased in the Upf1 KO cells (Fig. 2K,L). These data suggest that Upf1 triggers NMD of the *Mef2a* transcript, resulting in the downregulation of Mef2a expression. Thus, our results imply that Upf1 suppresses Arc expression, at least in part, by enhancing destabilization of *Mef2a* mRNAs, resulting in decreased Mef2a protein levels in neuronal cells.

Arc mRNA escapes from NMD

Because *Arc* has a long 3′UTR that contains two introns, it is thought that *Arc* mRNA is a natural target of NMD (Giorgi et al., 2007). Consistent with this, RNA interference (RNAi)-mediated knockdown of the NMD regulator Upf1 increases the level of *Arc* mRNA and protein in PC12 cells. To independently confirm whether Upf1 is involved in the regulation of *Arc* mRNA stability, we measured the half-life of endogenous *Arc* transcript in Upf1 knockdown N2a cells. Notably, despite an almost 3-fold increase in *Arc* mRNA steady-state levels (Fig. 1C) in cells with the Upf1 knockdown, the measured difference in actual mRNA stability in knockdown versus control cells was not statistically significant (Fig. S2A). This suggests that Upf1 affects this particular target mostly at the level of transcription, rather than mRNA stability. To rule out the possibility that our results were influenced by low residual levels of the Upf1 protein, we used Upf1 KO cells obtained with the CRISPR/Cas9 system. Consistent with previous results, the *Arc* mRNA half-lives in Upf1 KO and WT cells were found to be approximately equal (Fig. 3A). An additional test of mRNA stability involving qRT-PCR with specific primers targeting the *Arc* pre-mRNA also did not show any significant differences in mRNA decay in Upf1 KO versus WT cells (Fig. S2B).

We then developed a luciferase reporter assay based on the *Arc* 3′ UTR to determine whether the NMD surveillance pathway functions normally to control *Arc* gene expression. We built and tested two different *Arc* 3′UTR reporter constructs. In the first design, we inserted the *Arc* 3′UTR derived from genomic DNA (*Arc* 3′U-G), which contains two short introns, downstream of Renilla luciferase of psiCHECK2 vector (Fig. 3B). The EJC binds to this *Arc* 3′U-G after splicing occurs, and that spliced mRNA might be susceptible to degradation by NMD. We observed decreased luciferase mRNA levels from the reporter containing *Arc* 3′U-G, compared with the psiCHECK2 mock vector (Fig. 3C), but, surprisingly, we also found decreased reporter mRNA levels in Upf1 KO compared with WT cells (Fig. 3F). These results suggest the possibility that *Arc* mRNA becomes unstable through other novel mechanisms. To test this hypothesis, we inserted the complementary DNA (cDNA)-type *Arc* 3′UTR (*Arc* 3′U-C) into our reporter (Fig. 3D), and also observed decreased luciferase mRNA levels from the reporter containing *Arc* 3′U-C, compared with the control reporter (Fig. 3E). Moreover, we found that Upf1 deficiency did not significantly enhance the levels of *Arc* 3′U-C reporter mRNA (Fig. 3F). We next measured luciferase activity from this construct, compared with the *Arc* 3′U-G. Interestingly, the *Arc* 3′U-C reporter showed a decrease in luciferase activity when compared with control reporters lacking 3′UTR sequences (Fig. S2C,D); however, activity from this construct was not significantly different from that of the *Arc* 3′U-G reporter. Together, these results suggest that Upf1 does not act on the *Arc* 3′UTR to regulate the stability of this RNA transcript.

Journal of Cell Science (2019) 132, jcs224055. doi:10.1242/jcs.224055

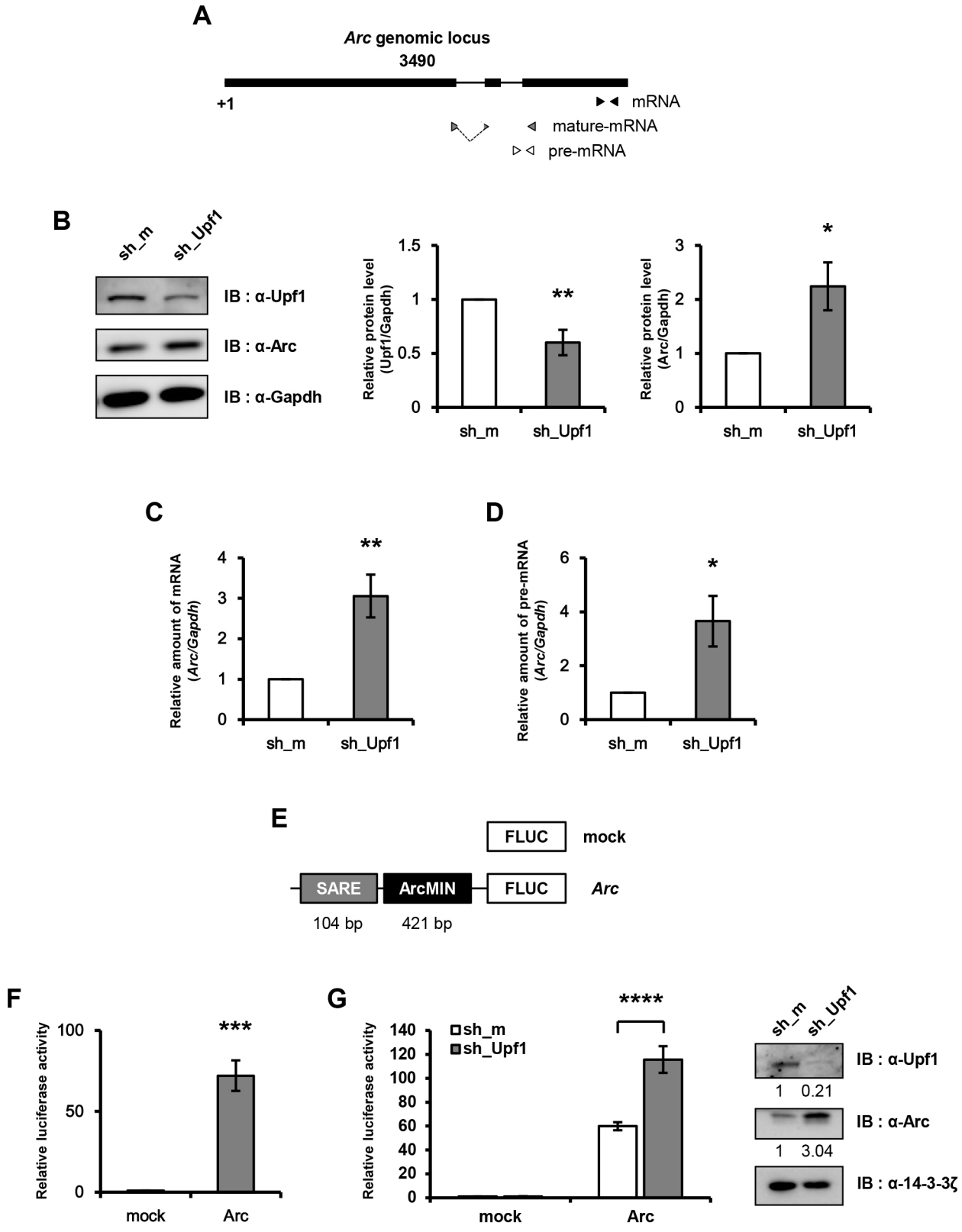

Fig. 1. See next page for legend.

Ago2 contributes to CBP80/20-dependent translation of *Arc* mRNA

Previous studies have shown that artificial tethering or loading of Ago2 onto the 3′UTR of premature termination codon (PTC)-containing mRNAs inhibits CBP80/20 (also known as NCBP1/2)-dependent translation efficiency and NMD (Choe et al., 2011, 2010). Ago2-mediated NMD inhibition is also dependent on the ability of Ago2 to associate with the cap

Journal of Cell Science (2019) 132, jcs224055. doi:10.1242/jcs.224055

Fig. 1. Depletion of Upf1 stimulates *Arc* gene transcription. (A) Schematic of the mouse *Arc* locus and primers used for quantitative RT-PCR (qRT-PCR). Exons are represented by boxes, and introns are shown as lines. (B) Immunoblots for Upf1 in Neuro-2a (N2a) cells transfected with mock shRNA (sh_m) or shRNA targeting *Upf1* (sh_Upf1) at 48 h post-transfection. *Gapdh* was used as a loading control. Numbers indicate densitometric values determined by Upf1/Gapdh or Arc/Gapdh ratios. The average value of densitometry in sh_m was set to 1 (unpaired two-tailed Student's *t*-test, $n=5$; *$P<0.05$, **$P<0.01$). (C,D) Levels of the mature (C) and premature (D) *Arc* mRNA were measured by qRT-PCR. Values are means±s.e.m. (unpaired two-tailed *t*-test, $n=5$; *$P<0.05$, **$P<0.01$). (E) Schematic description of the synaptic activity-responsive element (SARE)-TATA-containing short promoter of the *Arc* gene (ArcMin) reporter vector. SARE was fused directly upstream of ArcMin, a TATA-containing sequence near the *Arc* gene transcription initiation site. (F) The *Arc* promoter reporter replicates activation of the endogenous *Arc* gene. Firefly luciferase activity was normalized to Renilla luciferase activity, and mock luciferase activity was set to 1 (unpaired two-tailed Student's *t*-test, $n=4$; ***$P<0.001$). (G) Enhancement of *Arc* promoter activity under conditions of *Upf1* silencing. Knockdown of Upf1 was confirmed by immunoblotting. The numbers below the blot show the fold change relative to sh_m. The amount of Upf1 or Arc was normalized to 14-3-3ζ (two-way ANOVA with Sidak's multiple comparisons, $n=4$; ****$P<0.0001$). sh_m, short hairpin RNA_mock; sh_Upf1, short hairpin RNA_Upf1.

structure. In this manner, microRNAs (miRNAs) could serve as a surveillance system against nonsense codon-containing mRNAs. To test the possibility that this system is involved in *Arc* mRNA regulation, we first measured endogenous *Arc* mRNA levels in cells with knockdown of known miRNA-processing enzymes. Specifically, a small interfering RNA (siRNA) knockdown approach was used to downregulate expression of Ago2, Dicer (also known as Dicer1) and Drosha, key proteins required for miRNA biogenesis and function, and we found that downregulation of any one of these destabilizes *Arc* mRNA levels (Fig. 4A,B; Fig. S2E–G). To obtain more direct evidence for the regulatory role of miRNAs on *Arc* mRNA regulation, we verified an interaction between the *Arc* 3′UTR and Ago2 by streptavidin-biotin RNA affinity purification analysis. Overexpressed green fluorescent protein (GFP)-Ago2 was co-precipitated with biotin-labeled *Arc* 3′UTR mRNA (Fig. 4C). In contrast, 3′UTR-bound Ago2 was dramatically decreased by the addition of unlabeled *Arc* 3′UTR, suggesting that Ago2 specifically interacts with the 3′UTR of *Arc*. Endogenous Ago2 is also bound by the biotin-labeled full-length *Arc* 3′UTR, and its specific binding to *Arc* 3′UTR was confirmed by competition analysis with unlabeled 3′UTR (Fig. 4D). Interestingly, we found that CBP20 binding to *Arc* mRNA was significantly increased in Ago2 knockdown cells, suggesting that Ago2 inhibits CBP80/20-dependent translation of *Arc* mRNA (Fig. 4E). Collectively, these results suggest that Ago2 binds to the *Arc* 3′ UTR and could serve as a surveillance system to protect against NMD through CBP80/20-dependent translation efficiency.

Upf1 binds to *Arc* mRNA and suppresses its translation

Our measurement of endogenous *Arc* mRNA turnover rates and mRNA levels of the *Arc* 3′UTR reporter construct indicated that Upf1 was not a major determinant of *Arc* mRNA stability (Fig. 3). Therefore, we next tested whether Upf1 can bind to the *Arc* 3′UTR by performing RNA pulldown assays; our data confirmed that Upf1 can bind to *Arc* 3′UTR, and this binding was independent of the EJC (Fig. S3A). The 3′UTR also contains a repository of regulatory elements for translation. Previously, we demonstrated that the 3′ UTR of chryptochrome 1 (*Cry1*) was important for its rhythmic translation, and binding of AU-rich element RNA-binding protein 1 (Auf1; also known as Hnrnpd) to the *Cry1* 3′UTR recruits the 40S ribosomal subunit to the 5′ end of mRNA (Lee et al., 2014). To determine whether Upf1 similarly modulates *Arc* translation via binding to the *Arc* mRNA 3′UTR, we used the same reporter vectors containing the complete *Arc* 3′UTR from genomic DNA (*Arc* 3′U-G) or the *Arc* 3′UTR from cDNA (*Arc* 3′U-C) from previous experiments, as well as the negative-control vector psiCHECK2 mock (Fig. 5A, schematic). Interestingly, luciferase activities produced from both *Arc* 3′UTR-containing reporter constructs were enhanced in Upf1 KO cells, suggesting that Upf1 suppresses translation of *Arc* through its 3′UTR (Fig. 5A).

To confirm the role of Upf1 in translation of endogenous *Arc* mRNA, we applied sucrose gradient analysis to monitor the association of *Arc* mRNA with polysomes and non-polysomes in Upf1 KO or WT cells. We found that the overall ribosome profiles were similar in Upf1 KO and WT cells (Fig. 5B). Additionally, Upf1 KO did not affect the distribution of the control ribosomal protein L32 (*Rpl32*) mRNA. Critically, however, the distribution of *Arc* mRNA was shifted from the monosome to the polysome fraction in Upf1 KO cells, reflecting an induction of *Arc* mRNA translation (Fig. 5C; Fig. S3B). To further assess the potential translation-suppressing activity of Upf1, we transfected N2a cells with an mRNA reporter construct containing the *Arc* 3′UTR fused to luciferase containing an m^7GpppG-cap (Fig. 5D). We observed that luciferase synthesis from the *Arc* 3′UTR-containing reporter was considerably higher in Upf1 KO cells than in WT cells (Fig. 5E; Fig. S3C,D).

To clarify the mechanism involved in the Upf1-mediated translational regulation of *Arc*, we measured Ago2-binding affinities to the *Arc* 3′UTR in WT and Upf1 KO cells, because Ago2 was proposed to have a role in *Arc* translational regulation as described above (Fig. 4). Importantly, Ago2 binds more weakly to the *Arc* 3′UTR and, subsequently, increased CBP20 binding in Upf1 KO cells, suggesting that RNA helicase Upf1 regulates Ago2-binding affinity to the *Arc* mRNA and subsequent Ago2-mediated *Arc* translation (Fig. S4A,B). Next, we tested whether newly synthesized Arc in neuronal cells is induced by Upf1 depletion using a puromycin-proximity ligation assay (Puro-PLA) followed by immunostaining. The number of Arc Puro-PLA puncta increased in Upf1 KO compared with WT cells (Fig. 5F). Then, we tested whether newly synthesized Arc exploited 3′UTR-mediated translation mechanism. To this end, we prepared a vector that was designed to express the FLUC peptide under *Arc* 3′UTR (Fig. 5G) and either FLUC mock or *Arc* 3′UTR, which were co-transfected with EGFP vectors into WT or Upf1 KO cells prior to puromycin treatment of the cells. As expected, FLUC-Arc 3′U Puro-PLA puncta were increased in Upf1 KO compared with WT cells. However, there were no differences between Upf1 KO and WT cells in FLUC-mock Puro-PLA puncta (Fig. 5H,I; Fig. S4C,D). Taken together, these results imply that Upf1 induces translational repression by facilitating Ago2 binding towards 3′UTR of *Arc* mRNA.

Reduction of Upf1 expression leads to abnormal neurite outgrowth and branching

As shown in a previous study by Messaoudi et al. (2007), sustained translation of newly induced *Arc* mRNA is necessary for Cofilin (also known as Cfl1) phosphorylation. Given the evidence supporting a role for Upf1 in Arc expression, we next tested the level of phosphorylated (p)-Cofilin in Upf1 KO cells. Western blot analyses indicated that, as expected, Cofilin phosphorylation was robustly increased in Upf1 KO cells (Fig. 6A). Cofilin is one of the major regulators of F-actin dynamics, which controls actin polymerization as well as depolymerization (Bamburg and Bernstein, 2010). Its phosphorylated state promotes actin polymerization. Thus, regulation

Journal of Cell Science (2019) 132, jcs224055. doi:10.1242/jcs.224055

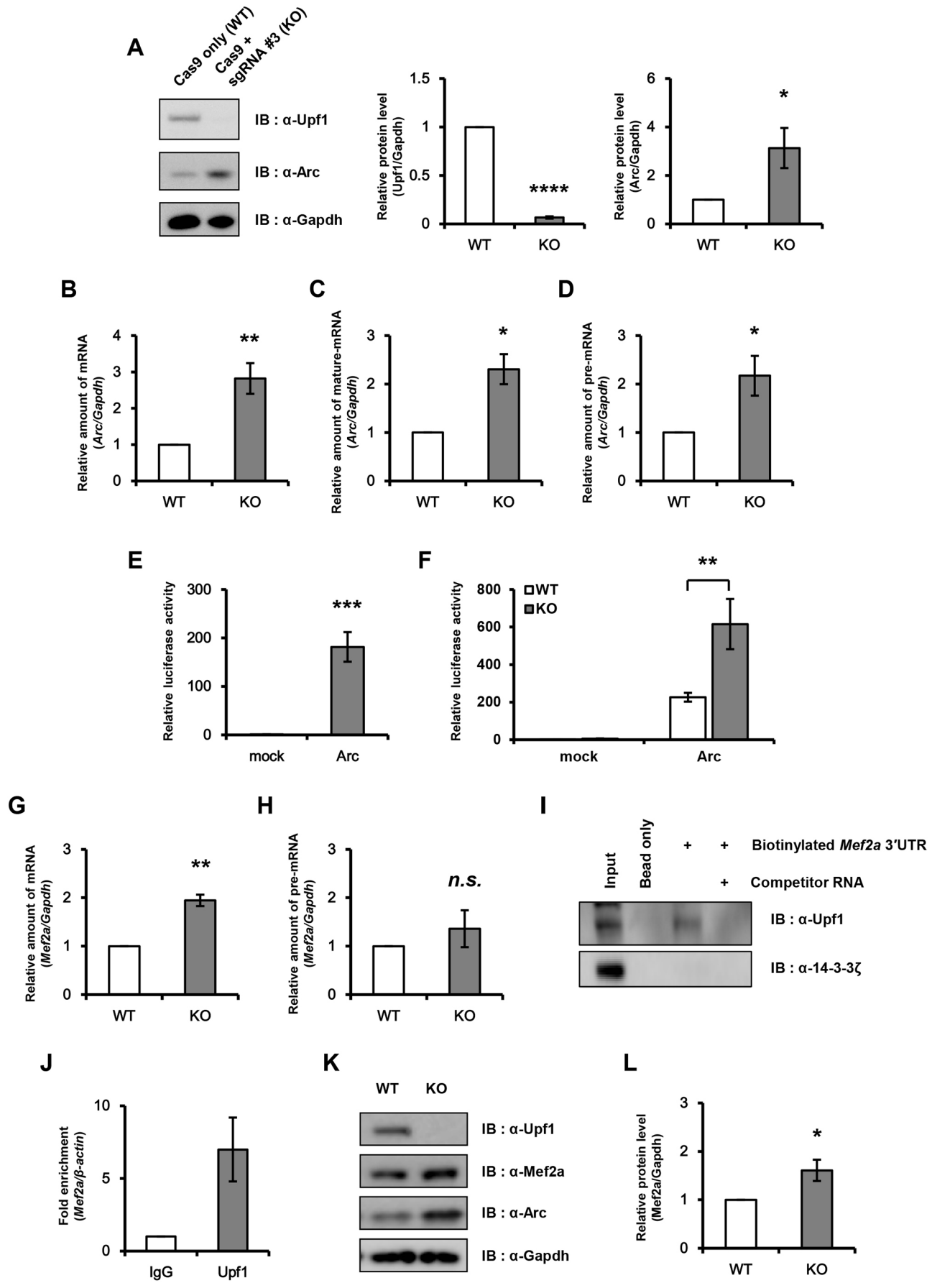

Fig. 2. See next page for legend.

Journal of Cell Science (2019) 132, jcs224055. doi:10.1242/jcs.224055

Fig. 2. CRISPR/Cas9-mediated Upf1 KO increases *Arc* transcriptional activity. (A) Upf1 KO using CRISPR/Cas9 was confirmed by immunoblotting with the indicated antibodies. Lysates from WT and Upf1 KO cells were probed with anti-Upf1 and anti-Arc antibodies. Upf1 protein is absent and total Arc protein abundance is increased in Upf1 KO cell lines. Numbers indicate densitometric values determined by Upf1/Gapdh or Arc/Gapdh ratios. The average value of densitometry in WT was set to 1 (unpaired two-tailed Student's *t*-test, n=4; *P<0.05, ****P<0.0001). (B–D) Levels of the total (B), mature (C) and premature (D) *Arc* mRNA were measured by qRT-PCR. Values are means±s.e.m. (unpaired two-tailed Student's *t*-test, n=3–6; *P<0.05, **P<0.01). (E) Luciferase assay to measure activity from the *Arc* promoter in N2a cells. Relative luciferase activities were compared with those from cells containing the pGL3 vector (mock) (unpaired two-tailed Student's *t*-test, n=5; ***P<0.001). (F) Enhancement of *Arc* promoter activity in Upf1 KO cells (two-way ANOVA with Sidak's multiple comparisons, n=5; **P<0.01). (G,H) Levels of the total (G) and premature (H) *Mef2a* mRNA were measured by qRT-PCR. Values are means±s.e.m. (unpaired two-tailed Student's *t*-test, n=3; n.s., not significant; **P<0.01). (I) Biotin-RNA pulldown indicated that Upf1 was capable of binding the 3′ untranslated region (UTR) of *Mef2a* mRNA in N2a cells. (J) Endogenous Upf1 binds to endogenous *Mef2a* mRNA. Lysates from N2a cells were used for RNA immunoprecipitation (RNA-IP) analysis using IgG and anti-Upf1 antibodies. RNA abundance in IP samples was determined by qRT-PCR. The levels of *Mef2a* mRNA were normalized to β-actin mRNA levels. Bars represent means±s.e.m. (n=3). (K) Western blotting was performed with the indicated antibodies. Mef2a protein levels are increased in Upf1 KO cells. (L) Calculated ratio of Mef2a/Gapdh protein levels. Data are shown as mean±s.e.m. (unpaired two-tailed Student's *t*-test, n=7; *P<0.05).

of Cofilin activity is critical in actin dynamics, which alters cell morphology and neuronal outgrowth. Interestingly, compared with WT cells, Upf1 KO cells generated longer neurite-like processes under normal conditions (Fig. 6B), indicating that the Upf1-dependent Arc regulation is essential for appropriate neurite outgrowth. Neurite outgrowth is a fundamental neural process in formation of proper neuronal connections in the central nervous system. Abnormal or excessive connections between neurons contribute to many neurodevelopmental diseases (Belmonte et al., 2004). We, hence, examined the effect of Upf1 on neurite outgrowth in primary hippocampal neurons. To examine the role of Upf1 in hippocampal neurons, we used shRNA encoding GFP and shRNA targeting *Upf1*. Two days after transfection on hippocampal neuron cultures, levels of Upf1 were significantly decreased compared with levels in neurons transfected with a mock shRNA, as measured by immunofluorescence (Fig. 6C,D). By analyzing individual neurons, we confirmed that neurons with Upf1 knockdown exhibited increased neurite length and number of primary branches compared with mock shRNA-transfected neurons (Fig. 6E–G). Concordantly, the results from Sholl analysis clearly showed that dendritic arborization was enhanced in shRNA targeting *Upf1* (sh_Upf1)-transfected neurons, suggesting that Upf1 is required for proper neurite outgrowth and branching (Fig. 6H,I).

DISCUSSION

A novel function for Upf1 in transcriptional suppression of *Arc*

Genome-wide microarray and RNA-seq expression analyses have suggested a regulatory role for Upf1 (Mendell et al., 2004; Pan et al., 2006). However, most studies aimed at identifying Upf1 targets have not distinguished Upf1 indirect versus direct targets. In a previous investigation, whole-transcriptome decay rates were measured in Upf1-depleted cells using a combined RNA-seq and BRIC-seq approach (Tani et al., 2012). This analysis identified 76 direct Upf1 target transcripts that show altered decay rates and are upregulated in Upf1-depleted cells. Interestingly, however, hundreds of transcripts were at least 2-fold upregulated, but did not show altered decay rates, in response to Upf1 depletion. These transcripts were referred to as indirect NMD targets. Another study involving the simultaneous analysis of pre-mRNA and mRNA abundance for an array of selected transcripts strongly suggested that Upf1 depletion promotes transcriptional activation (Viegas et al., 2007). That is, a subset of 16 transcripts was affected by Upf1 depletion in an NMD-independent and non-post-transcriptional fashion. The results of our study are consistent with these data and indicate that Arc expression is also regulated by Upf1 at the level of transcription.

We first analyzed *Arc* mRNA and pre-mRNA levels in Upf1 knockdown and KO cells by qRT-PCR and found that these did not differ significantly (Figs 1C,D and 2B–D), strongly suggesting that *Arc* mRNA is transcriptionally modulated. The *Arc* promoter has been well characterized and is widely used as a tool to facilitate neuronal activity mapping (Kawashima et al., 2009; Waltereit et al., 2001). In addition, this promoter has been employed to successfully track an active neuronal circuit in living mice (Kawashima et al., 2013). Here, we utilized an *Arc* promoter-luciferase reporter to investigate the potential for gene expression at the transcriptional level by Upf1. Consistent with our results measuring endogenous transcripts, *Arc* promoter activity was found to be upregulated in Upf1-depleted cells (Figs 1G and 2F).

The transcription factors Mef2a and Mef2d are highly expressed in the brain and are tightly regulated by several distinct calcium signaling pathways (McKinsey et al., 2002). These Mef2 transcription factors negatively regulate excitatory synapse number in an activity-dependent manner, in part, through the induction of *Arc* transcription (Flavell et al., 2006). Here, we found that Upf1 binds to endogenous *Mef2a* mRNA, and both *Mef2a* mRNA and protein levels are significantly elevated in Upf1 KO cells (Fig. 2G–L). This suggests that Upf1 can modulate Arc levels indirectly via its effect on Mef2a.

The length of the 3′UTR has been suggested as an important feature that influences NMD, and a number of studies have shown that long 3′UTRs strongly promote NMD and increase Upf1 assembly in targeted mRNAs (Hogg and Goff, 2010; Hurt et al., 2013; Yepiskoposyan et al., 2011). It has further been found that the 3′UTRs of Upf1 indirect target transcripts (group A mRNAs) are significantly longer than those of other transcripts (Tani et al., 2012). Here, we demonstrated that a 3719-nucleotide (nt) region at the 3′UTR of *Mef2a* is critical for NMD (Fig. S5A). A recent study identified important features of 3′UTRs targeted by Upf1 and found that these have GC-rich motifs embedded in high GC-content regions (Imamachi et al., 2017). Notably, the *Mef2a* 3′UTR contains one such GC-rich motif (Fig. S5A, highlighted in red). We further showed *Arc* promoter activity using Mef2a knockdown to establish a causal mechanism (Fig. S5B). Consistent with this observation, transcription factors were enriched among potential Upf1 targets (Imamachi et al., 2017), and, indeed, several transcription factors, including activating transcription factor 3 (ATF3) and CAMP response element-binding protein 2 (Creb2; also known as ATF4), have been identified as Upf1 targets (Mendell et al., 2004). The SARE located upstream of the *Arc* gene is a major neuronal activity-dependent element, which consists of binding sites for Creb, Mef2 and serum response factor (Srf) proteins. As expected, and consistent with our previous results, gene expression profiles for *Creb2* obtained in Upf1 KO cell lines indicated that this transcript is also regulated by Upf1 (Fig. S5C).

Regulation of gene transcription is one of the main mechanisms for modulating the levels of specific mRNAs and proteins. Both the selective localization and accumulation of *Arc* mRNA at synapses

Journal of Cell Science (2019) 132, jcs224055. doi:10.1242/jcs.224055

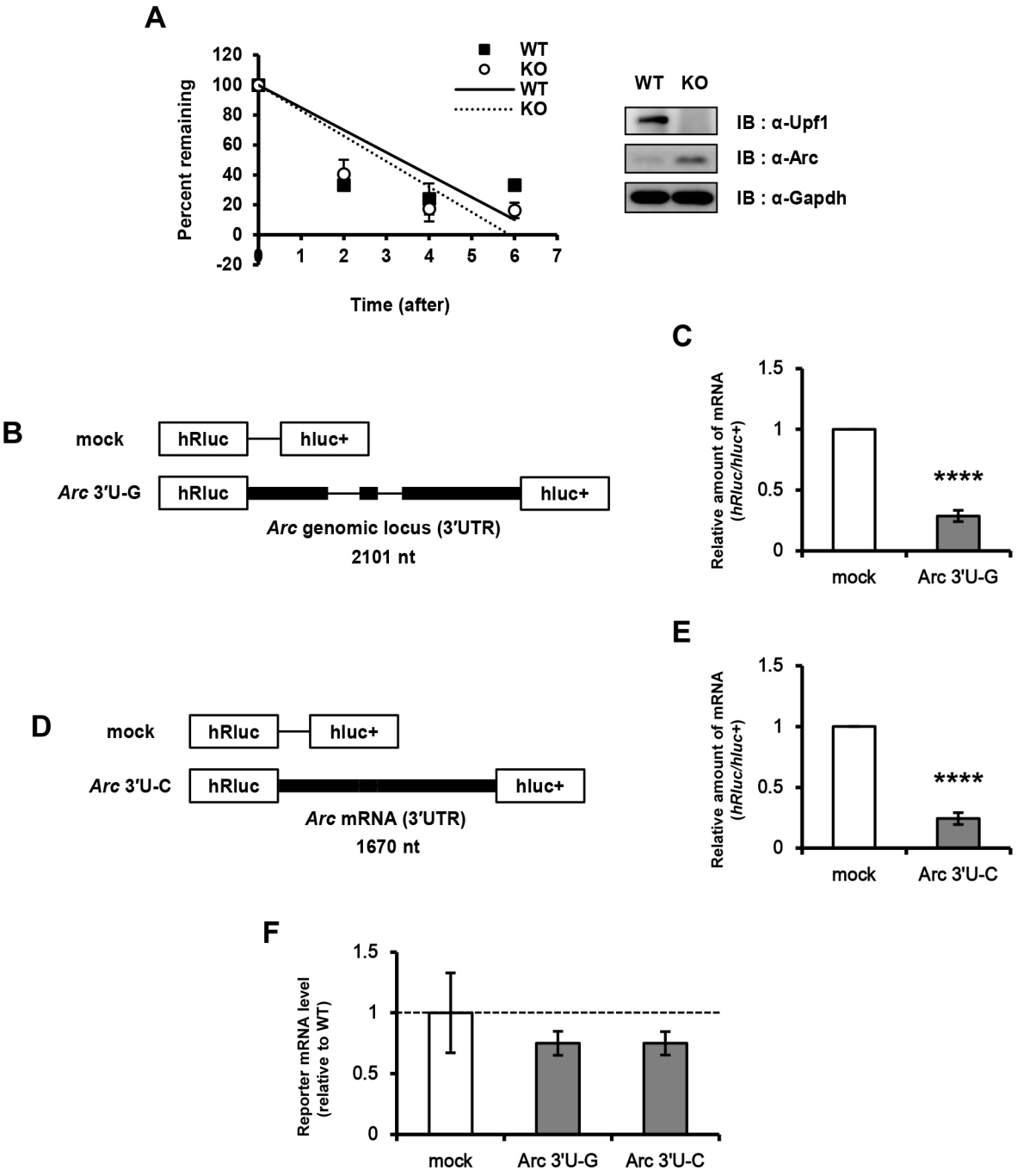

Fig. 3. The stability of *Arc* mRNA is not affected by inhibition of nonsense-mediated mRNA decay (NMD). (A) *Arc* mRNA levels after 2, 4 and 6 h of 5,6-dichloro-1-beta-D-ribofuranosylbenzimidazole treatment are shown as percentages on the *y*-axis (n=3). (B) Schematic drawing of reporter gene constructs. Reporter construct composed of the psiCHECK2-backbone plasmid encoding the Renilla luciferase gene and containing the mouse genomic 3′UTR of *Arc* (*Arc* 3′U-G). (C) Relative mRNA levels in N2a cells transfected with mock or the *Arc* 3′U-G construct were determined by qRT-PCR (unpaired two-tailed Student's *t*-test, n=4; ****P<0.0001). (D) Schematic representation of reporter containing the 3′UTR of *Arc* from mouse cDNA (*Arc* 3′U-C). (E) Relative mRNA levels in N2a cells transfected with mock or the *Arc* 3′U-C construct were determined by qRT-PCR (unpaired two-tailed Student's *t*-test, n=4; ****P<0.0001). (F) Relative reporter mRNA levels in WT or Upf1 KO cells (n=6). The level of reporter mRNAs was normalized by KO/WT ratios, and mock luciferase mRNA was set to 1.

are mediated by activity-dependent regulation of this transcript throughout dendrites (Farris et al., 2014; Steward et al., 1998). These findings suggest that differential localization of *Arc* mRNA is the combined result of targeting newly synthesized *Arc* mRNA to active domains and degradation throughout dendrites in the hippocampus. When transcription is inhibited, there is no accumulation of *Arc* mRNA in the activated lamina, although *Arc* mRNA was already present throughout dendrites. In this study, we provide evidence for a novel role for Upf1 in the precise regulation of *Arc* transcription, which we propose allows for a more exquisite activity-dependent control of Arc expression.

Role of Ago2 in NMD of *Arc* mRNA

One-third of human genes have 3′UTRs longer than 1000 nts (Pesole et al., 2000). This raises the question of how a large subset of naturally occurring mRNAs containing long 3′UTRs have acquired

Journal of Cell Science (2019) 132, jcs224055. doi:10.1242/jcs.224055

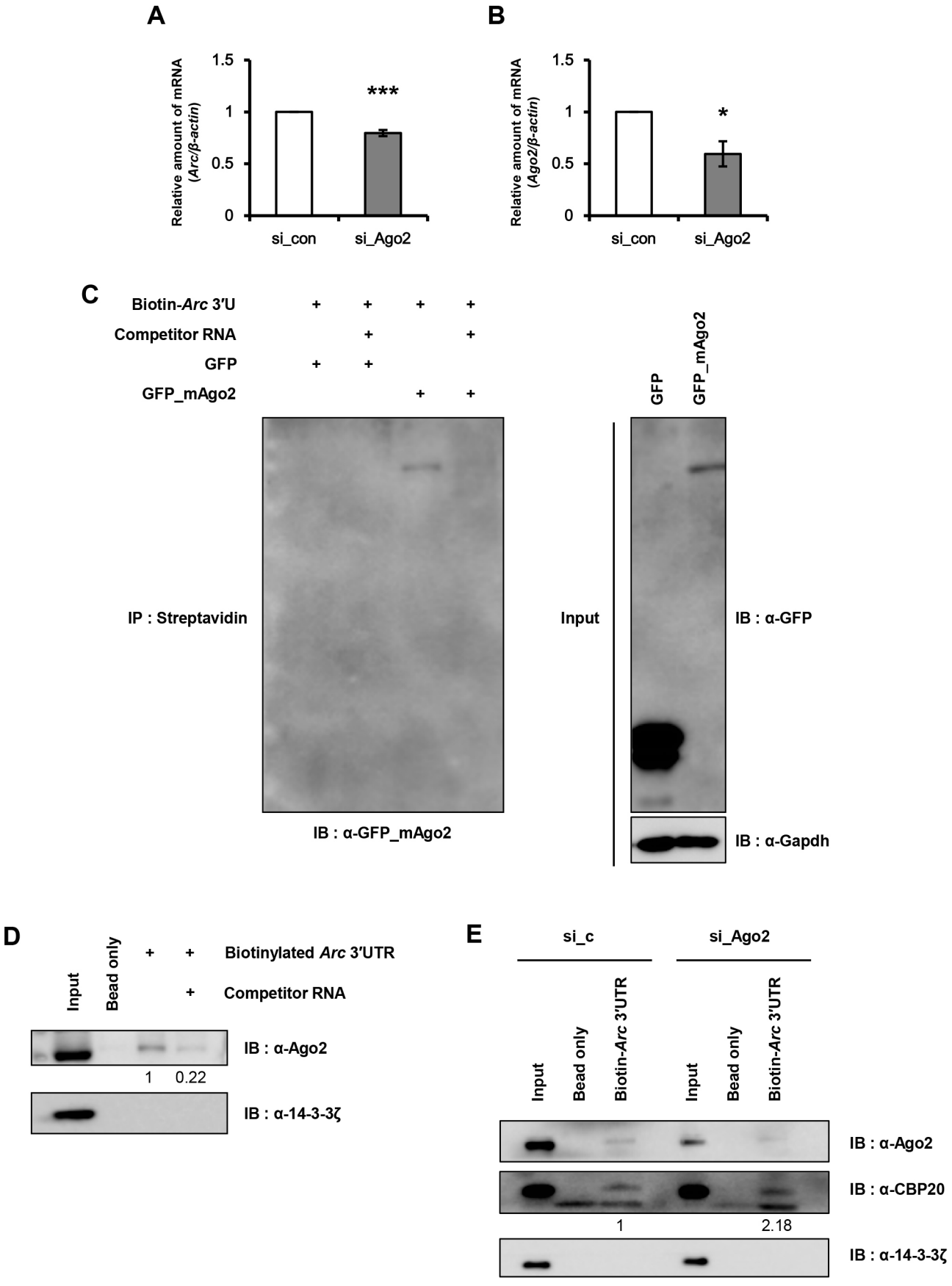

Fig. 4. See next page for legend.

Journal of Cell Science (2019) 132, jcs224055. doi:10.1242/jcs.224055

Fig. 4. Ago2 regulates *Arc* mRNA levels by binding to the 3′UTR. (A,B) The relative mRNA levels of *Arc* (A) and *Ago2* (B) were quantified by qRT-PCR and normalized to β-actin mRNA levels (unpaired two-tailed Student's *t*-test, $n=5$; *$P<0.05$, ***$P<0.001$). (C,D) The *in vitro*-transcribed *Arc* 3′UTR construct was labeled with biotin-UTP and incubated with cell lysates from GFP-mAgo2-overexpressing N2a cells (C) or untreated N2a cells (D). For competition assay, non-labeled *Arc* 3′UTR (10×) was also co-incubated. Streptavidin affinity-purified samples were separated by SDS-PAGE and subjected to immunoblot analysis with the indicated antibodies. The numbers below the blot show the fold change relative to biotinylated *Arc* 3′UTR only. (E) *In vitro*-transcribed biotin-*Arc* 3′UTR was incubated with cell lysates from si_c- or si_Ago2-treated N2a cells. CBP20 binding was measured by immunoblotting. The numbers beneath the blot show the fold change relative to biotinylated *Arc* 3′UTR only in si_c. 14-3-3ζ was used as a loading control and negative control.

mechanisms to evade the NMD pathway. A recent study identified a *cis*-acting element located within the first 200 nts of the 3′UTR, which inhibits NMD when positioned downstream of the translation termination codon (Toma et al., 2015). Additionally, binding of Ago2 to the 3′UTR of PTC-containing mRNAs abrogates NMD by inhibiting CBP80/20-dependent translation (Choe et al., 2011). Uniquely, *Arc* pre-mRNA contains two introns in the 3′UTR, strongly suggesting that this transcript is a natural target of NMD. To test whether the post-transcriptional decay of *Arc* mRNA occurs via NMD, we measured both endogenous *Arc* mRNA stability and the levels of an mRNA reporter construct containing the *Arc* 3′UTR region in cells depleted for Upf1, a critical component of the NMD pathway. Interestingly, we found that *Arc* mRNA stability was not increased in Upf1-depleted cells (Fig. 3A; Fig. S2A,B), and, similarly, *Arc* 3′UTR reporter mRNA levels were unaffected by Upf1 depletion (Fig. 3F; Fig. S2C,D).

It has previously been determined that coactivator-associated arginine methyltransferase 1 (Carm1) associates with the major NMD factor Upf1 and promotes its occupancy on PTC-containing transcripts (Sanchez et al., 2016). As predicted, growth arrest and DNA damage inducible alpha (*Gadd45a*) and asparagine synthetase (glutamine-hydrolyzing) (*Asns*), which are established NMD targets, show stabilized mRNA levels in Carm1 KO mouse embryonic fibroblasts (MEFs). Surprisingly, however, in the same study, *Arc* mRNA decay rates were found to be similar in Carm1 KO and WT MEFs. Moreover, other reports have suggested that some plant genes containing introns in their 3′UTR are not subject to NMD (Gadjieva et al., 2004; Rose, 2004). Here, we found that Ago2 binds to 3′UTR of *Arc*, and, interestingly, downregulation of this protein, as well as those involved in miRNA biogenesis, including Drosha and Dicer, results in reduced *Arc* mRNA levels (Fig. 4; Fig. S2E–G), suggesting that Ago2 might inhibit Upf1-mediated NMD. These data demonstrate that *Arc* is an endogenous Ago2-mediated surveillance target gene and thus provide evidence for the existence of a novel mechanism for post-transcriptional regulation of gene expression, involving regulation of NMD by miRNAs, in neuronal cells. It is reported that a set of miRNAs, which are predicted as binding candidates of *Arc* 3′UTR, inhibit Arc protein expression in cultured hippocampal neurons (Wibrand et al., 2012). A previous study identified differential regulation of Ago2-associated and Arc-targeting miRNA following LTP induction using Ago2 immunoprecipitation (IP) (Pai et al., 2014). Interestingly, Ago2 IP/input ratios of miR-34a were enhanced, but Ago2 IP/input ratios of miR-326 were significantly decreased, following high frequency stimulation. Given the central role of Arc expression in LTP, Ago2 might be a potential effector in synaptic plasticity.

NMD requires both splicing and translation, and the EJC also plays a critical role in this process. Here, we found that a reporter construct containing the cDNA-type *Arc* 3′UTR was destabilized to a similar extent as the intron containing *Arc* 3′UTR, indicating that *Arc* mRNA is degraded through a novel mechanism, distinct from NMD (Fig. 3D,E; Fig. S2C,D). This finding is also supported by the results of Ninomiya et al. (2016). To analyze the mechanism for human *ARC* mRNA degradation, the authors constructed an *ARC* genome-type 3′UTR fused to an EGFP reporter and then removed the termination codons, in order to inhibit NMD targeting of this construct. Surprisingly, however, termination codon removal from the *ARC* mRNA 3′UTR did not stabilize reporter mRNA. This implies a role for other mRNA decay processes in *ARC* mRNA regulation. Importantly, *ARC* mRNA localization is mediated by a dendritic-targeting element (DTE) in the *ARC* 3′UTR, which also has a *cis*-acting element for destabilizing *ARC* mRNA, independent of the NMD pathway (Ninomiya et al., 2016). Besides, this DTE alone was able to promote degradation of the reporter RNA, dependent on translation. In this study, we do not address the potential for additional *Arc* mRNA degradation and destabilization mechanisms, including *trans*-acting elements, and the identity of any *cis*- and *trans*-acting factors, as well as the region of the mouse *Arc* mRNA transcript required for degradation and binding of destabilizing factors, remains to be elucidated.

Upf1 suppresses *Arc* translation through its binding to 3′UTR

The 3′UTR contains regulatory elements that post-transcriptionally influence gene expression, and these regions can affect mRNA stability (Kim et al., 2011), localization and translation efficiency (Lee et al., 2014). It is thought that longer UTRs may contain regulatory motifs necessary to specify complex temporal and spatial translational regulation. *Arc* has a long 3′UTR, consisting of 1670 nts, so we tried to reveal another possible role for Upf1 in the translation of *Arc*. Additionally, the *Arc* mRNA 3′UTR region was reported to contribute to the modulation of Arc expression upon BDNF treatment (Paolantoni et al., 2018). By *in vitro* binding assay, we first confirmed that Upf1 binds to the 3′UTR of *Arc* regardless of the EJC, which shows the possible effects of Upf1 on post-transcriptional regulation of *Arc*. It is reported that the binding of Upf1 to the EJC triggers Upf1 phosphorylation, and phospho-Upf1 can mediate translational repression (Isken et al., 2008). Here, we demonstrated translational repression of *Arc* in the presence of Upf1 using a luciferase reporter activity analysis and polysome profiling of reporter mRNA (Fig. 5; Fig. S3A,B). Importantly, regardless of the presence of the EJC, binding of Upf1 to the *Arc* 3′UTR represses translation. LTP consolidation in the dentate gyrus of the hippocampus induced a shift in *Arc* mRNA from monosomes and messenger ribonuclearprotein particles to heavy polysomes (Panja et al., 2014). This shift in *Arc* mRNA may also be caused, in part, by the changes in the binding properties of Upf1 to *Arc* mRNA, although the specific mechanism underlying this effect is still to be found. Upf1 is widely recognized as an RNA helicase and, once recruited on target mRNAs, Upf1 can move along the mRNA to remodel the messenger ribonucleoproteins (Fiorini et al., 2015; Jankowsky, 2011). We showed that Ago2 also binds to 3′UTR of *Arc* and might inhibit *Arc* translation and NMD. To confirm the role of Ago2 in the Upf1-mediated translational repression of *Arc*, we evaluated Ago2-binding affinity to *Arc* 3′UTR in the presence or absence of Upf1. We found that the binding affinity of Ago2 to *Arc* 3′UTR was decreased in the Upf1 KO cells (Fig. S4A), which correlates with translational repression of *Arc* in the presence of Upf1. The discovery of numerous mRNA transcripts in dendrites has suggested that synapses could be modified directly through regulation of local protein synthesis (Bramham and Wells, 2007; Sutton and Schuman, 2006). It is thought that synaptic mRNAs are

Journal of Cell Science (2019) 132, jcs224055. doi:10.1242/jcs.224055

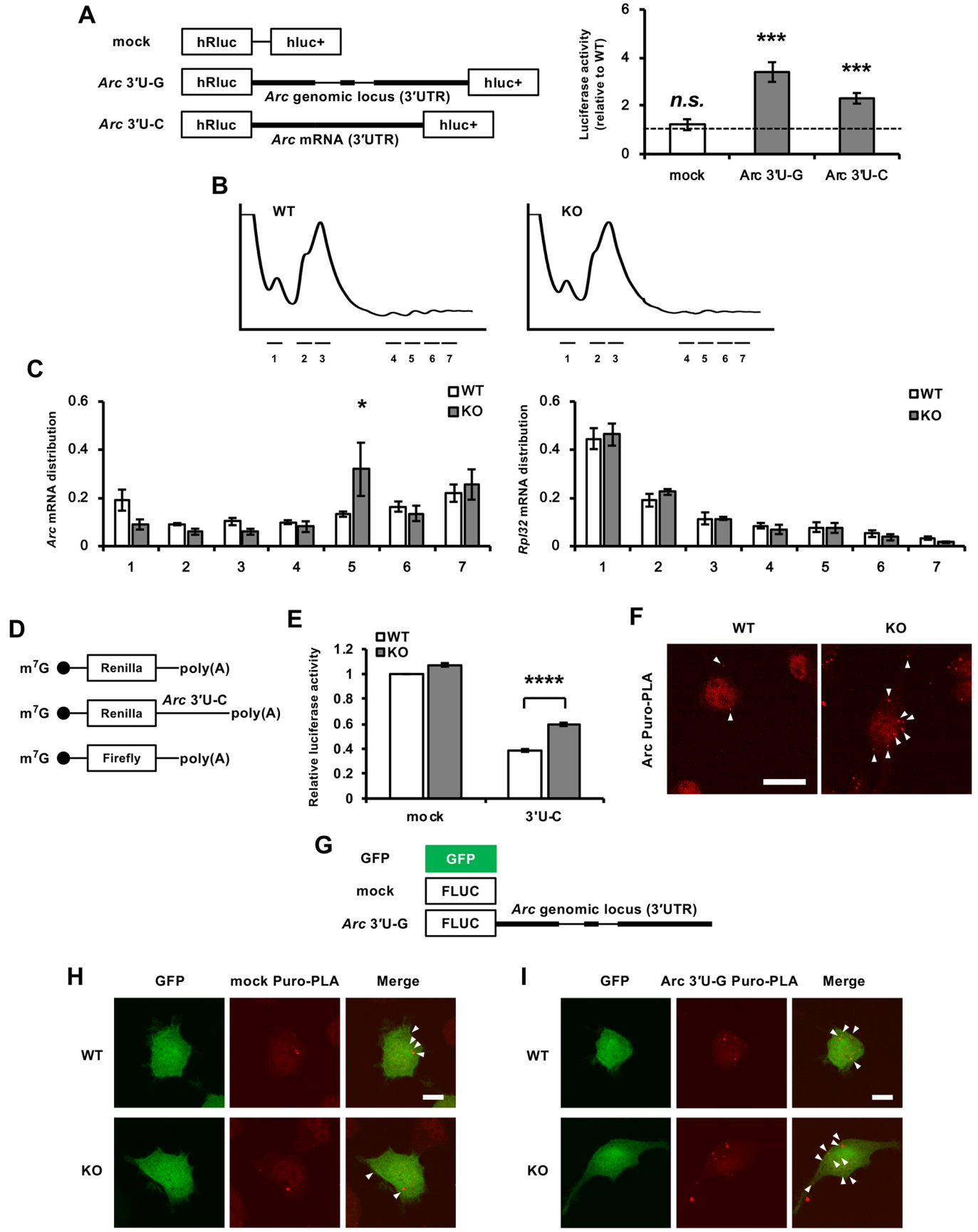

Fig. 5. See next page for legend.

Journal of Cell Science (2019) 132, jcs224055. doi:10.1242/jcs.224055

Fig. 5. Upf1 regulates translation of *Arc* mRNA. (A) Schematic representation depicting the psiCHECK2-derived reporters used for reporter gene assays (left). Levels of reporter activities as measured by analysis of genomic *Arc* 3′UTR (*Arc* 3′U-G) and cDNA *Arc* 3′UTR (*Arc* 3′U-C) luciferase reporters (right). Luciferase activity is shown as the ratio of hRluc to hluc+, and the luciferase activity from each reporter in WT cells was set as 1. Bars represent means±s.e.m. (unpaired two-tailed Student's *t*-test, $n=5$; n.s., not significant; ***$P<0.001$). (B) Polysome profiles of extracts from WT or Upf1 KO cells were determined from a UV monitor (254 nm). Polysome positions, as well as those corresponding to the 40S, 60S and 80S ribosomal subunits, are marked. (C) Polysome profiling fractions were pooled into seven larger fractions, containing 40S, 60S, 80S or polysome-bound RNA, ranging from lower to higher ribosome occupancy. *Arc* and *Rpl32* mRNA were quantified in each pooled fraction and normalized to an exogenous luciferase mRNA control. The ratio of total mRNA for each fraction was calculated. Error bars represent s.e.m. of four independent experiments (two-way ANOVA with Sidak's multiple comparisons; *$P<0.05$). (D) Schematic representation of the mRNAs measured in this experiment. Firefly mRNA reporters for normalization were also used. (E) Mock and *Arc* 3′U-C mRNAs synthesized *in vitro* by T7 RNA polymerase were transfected into WT and Upf1 KO cells using Lipofectamine 2000. After a 12-h incubation, luciferase assays were performed (two-way ANOVA with Sidak's multiple comparisons, $n=4$; ****$P<0.0001$). (F) Representative images of PLA signals on WT or Upf1 KO cells. To observe newly synthesized endogenous Arc proteins, puromycin-proximity ligation assay (Puro-PLA) was performed. Scale bar: 20 µm. White arrowheads highlight Puro-PLA signals in a single cell. (G–I) The indicated FLUC plasmids were co-transfected with GFP. After 24 h of transfection, Puro-PLA was performed and puromycin was treated for 90 min. The Puro-PLA method using a combination of anti-puromycin and anti-FLUC antibodies was able to detect newly synthesized FLUC. White arrowheads highlight Puro-PLA signals in a single cell. Scale bars: 10 µm.

transported in a translationally dormant state via interactions with RNA-binding proteins. Following synaptic stimulation, local mRNA translation is then activated in the synaptic region by neutralizing the repressive RNA-binding proteins. In our study, we found that *Arc* mRNA is not simply degraded by NMD. Rather, Upf1 suppresses *Arc* mRNA translation through regulation of Ago2-binding affinity towards the *Arc* 3′UTR, which may aid in precise spatiotemporal gene regulation.

Upf1-mediated *Arc* suppression regulates neurite extension

LTP and LTD typically require a rapid induction of gene expression. In *Arc* KO mice, early-phase LTP is enhanced, whereas late-phase LTP is blocked, and LTD, in general, is reduced (Plath et al., 2006). Synaptic depression in both homeostatic plasticity and LTD is mediated by AMPAR endocytosis. There is strong evidence for Arc involvement in excitatory synaptic transmission via interaction with components of the dynamin and endophilin 2/3 complex, which leads to internalization of surface AMPAR (Chowdhury et al., 2006; Park et al., 2008; Waung et al., 2008). It has also been found that knockdown of the EJC factor, eIF4AIII, increases *Arc* mRNA and protein levels, which should decrease the levels of surface AMPAR at synapses. However, unexpectedly, eIF4AIII knockdown resulted in increased amounts of surface AMPAR (Giorgi et al., 2007).

Previous reports have suggested that Arc performs a dynamic function in LTP *in vivo* (Messaoudi et al., 2007). Initial Arc synthesis is necessary for early stages of LTP, whereas late synthesis is required to generate stably modified synapses. Local infusions of antisense oligodeoxynucleotides against Arc during LTP results in Cofilin dephosphorylation and the loss of F-actin from synaptic sites. Here, we show that a number of Upf1 KO N2a cells have neurite-bearing morphology (Fig. 6B), and these structural changes suggest the possibility that Upf1-mediated Arc regulation affects F-actin expansion. Importantly, sustained hyperphosphorylated Cofilin can be observed in Upf1 KO cells, as shown in Fig. 6A, and we also tested whether Arc knockdown blocks the increase in Cofilin phosphorylation (Fig. S6A).

Our work reveals a physiological role of the Upf1-mediated *Arc* gene expression in controlling neurite outgrowth and dendritic branching (Fig. 6E–I), which are critical processes for proper wiring of the complex neuronal networks in the brain.

Conclusions

In this study, we provide evidence that Upf1 suppresses *Arc* transcription and translation via a number of distinct mechanisms. At the transcriptional level, Upf1 regulates *Arc* activity indirectly by regulating the transcription factors Mef2a and Creb2. Additionally, Upf1 suppresses *Arc* mRNA translation through its binding to the *Arc* 3′UTR, although *Arc* transcripts, which had been thought to be targeted for NMD, escape from this pathway and are stabilized by miRNA-mediated gene silencing. Finally, we show that depletion of Upf1, which leads to sustained Arc expression, promotes hyperphosphorylation of Cofilin and triggers neurite extension. Thus, based on these data, we propose that the Upf1-mediated downregulation of Arc at the level of transcription and translation in basal conditions is necessary for activity-induced Arc synthesis and subsequent activity-dependent changes in synaptic strength.

MATERIALS AND METHODS

Plasmid constructs

To generate psiCHECK2 *Arc* 3′U-C, mouse *Arc* (accession no. NM_018790.3) 3′UTR was amplified using Pfu polymerase (SolGent) with specific primers and the sequence was confirmed by sequencing. To generate psiCHECK2 *Arc* 3′U-G, *Arc* 3′UTR genomic DNA was amplified from Institute for Cancer Research (CrljBgi:CD-1) mice brain genomic DNA using the specific primers. For the *in vitro* binding analysis, full-length *Arc* 3′UTRs were amplified as previously described. PCR products were digested with specific enzymes *Eco*RI/*Xba*I and subcloned into pBluescript SK(+) (pSK) to generate pSK-*Arc* 3′U-G or -C.

Cell culture and drug treatment

N2a and NB41A3 cells were grown in Dulbecco's modified Eagle's medium supplemented with 10% heat-inactivated fetal bovine serum and 100 U/ml penicillin G and streptomycin. All cell lines were authenticated prior to experiments and they are not listed as commonly misidentified cell lines by the International Cell Line Authentication Committee. Cell identity and status are regularly checked. To block transcription, cells were treated with 5 µg/ml actinomycin D (Sigma-Aldrich, A9415) or 100 µg/ml 5,6-dichloro-1-beta-D-ribofuranosylbenzimidazole (Sigma-Aldrich, 53-85-0) and then harvested at the indicated time points. To block translation, cells were treated with 100 µg/ml cycloheximide (CHX; EMD Millipore, 239764).

Hippocampal cultures were prepared from embryonic day 17 mouse embryos and treated with DNase (Sigma-Aldrich, DN25) and trypsin (Sigma-Aldrich, T6567) at 37°C. Hippocampal primary neurons were seeded on 12-well plates with round glass coverslips or six-well plates without round glass coverslips coated with poly-L-lysine. Neurons were cultured in neurobasal medium (Gibco, Thermo Fisher Scientific, A3582901) with 1% glutamax (Gibco, Thermo Fisher Scientific, 35050061), 1% penicillin/streptomycin and B27 supplement (Gibco, Thermo Fisher Scientific, 17504044). Neurons at days *in vitro* (DIV)1 or DIV12 were transfected using Lipofectamine 2000 (Invitrogen) according to the manufacturer's protocol.

Generation of Upf1 KO cell lines

Generation of KO cell lines was performed as previously described (Lee et al., 2016; Mali et al., 2013). A 19 bp of the selected sequence (5′-TGCTCGGCGCCGACACCCA-3′) targeting the DNA region within exon 1 of *Upf1* was selected from *in silico* tools of predicted protospacer adjacent motif target sites. 5′-CTGCTCGGCGCCGACACCCAGGG-3′ was inserted into two 60-mer oligonucleotides (Insert_F, 5′-TTTCTTGGCTT-

Journal of Cell Science (2019) 132, jcs224055. doi:10.1242/jcs.224055

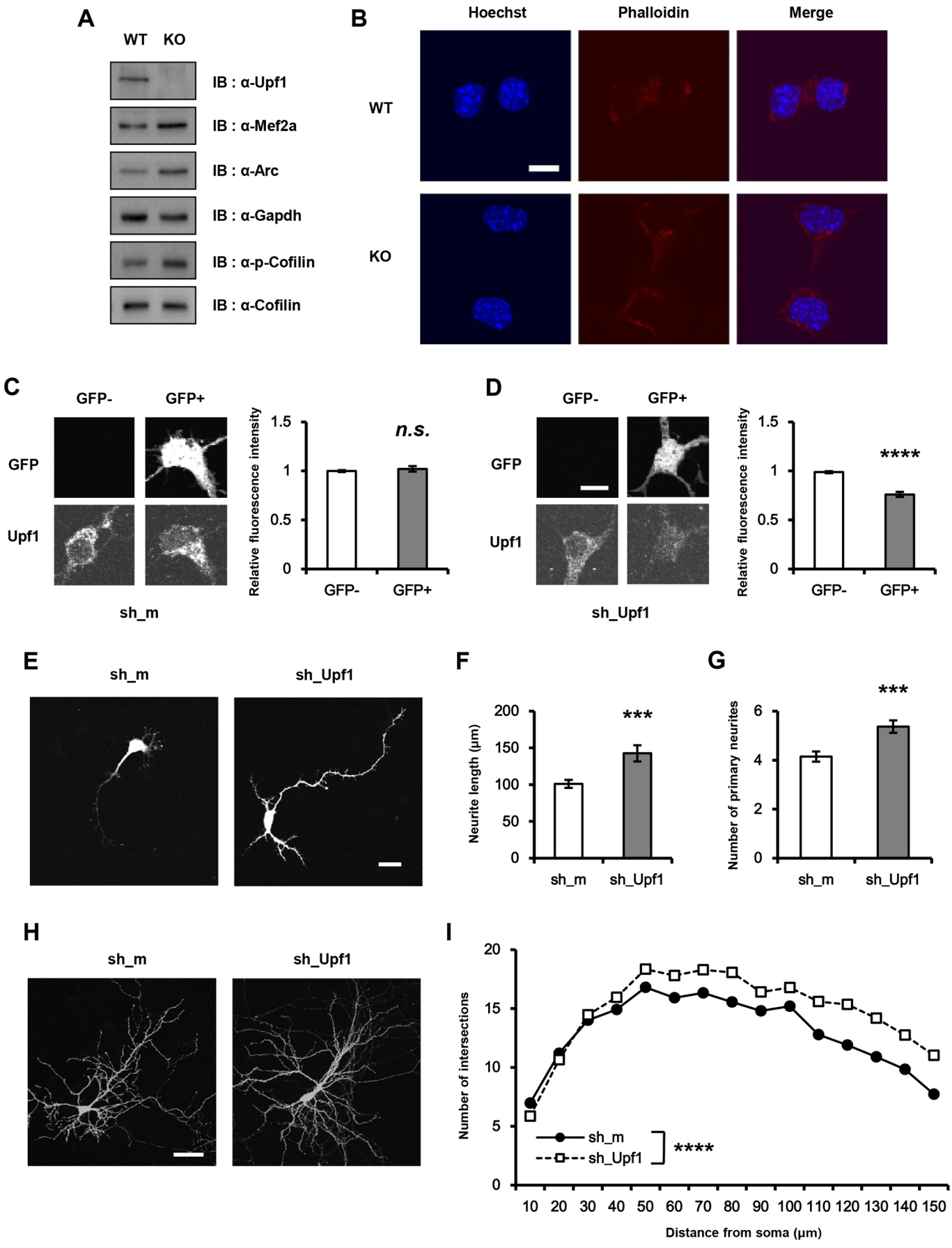

Fig. 6. See next page for legend.

Fig. 6. Upf1 regulates neurite outgrowth and branching of hippocampal neurons. (A) Immunoblots to measure levels of the indicated proteins in WT and Upf1 KO cells. (B) Representative images from WT and Upf1 KO cells are presented. WT or KO cells were labeled using fluorescent phalloidin. (C,D) Representative images (left) and quantitation (right) of Upf1 protein in neurons. sh_m or sh_Upf1 were transfected on DIV1 hippocampal neurons. After 48 h, Upf1 protein levels were confirmed by immunocytochemistry. Data are from 12 individual neurons from three independent experiments (unpaired two-tailed Student's *t*-test, n=23–84 neurons from four independent experiments; n.s., not significant; ****P<0.0001). (E–G) sh_m or sh_Upf1 were transfected to hippocampal primary neurons at DIV1, and neurite length and numbers of primary neurites at DIV3 were measured. Neurite length and number of primary neurites were significantly increased in neurons transfected with Upf1 shRNA (two-way ANOVA with Sidak's multiple comparisons, n=57–62 neurons from four independent experiments; ***P<0.001). Scale bar: 20 µm. (H) Representative neurons transfected with shRNAs. Scale bar: 50 µm. (I) Number of intersections of the dendrite at different distances (radius) from the soma (center of analysis) from Sholl analysis (two-way ANOVA with Sidak's multiple comparisons, n=35, 36 neurons; P<0.05 for 10, P<0.001 for 50, 90, 100 and ****P<0.0001 for 60, 70, 80, 110, 120, 130, 140, 150 µm distance from soma). All values represent mean±s.e.m.

TATATATCTTGTGGAAAGGACGAAACACCGNNNNNNNNNNNNNN-NNNNNN-3′ and Insert_R, 5′-GACTAGCCTTATTTTAACTTGCT-ATTTCTAGCTCTAAAACNNNNNNNNNN-NNNNNNNNNC-3′). The two oligonucleotides were annealed and extended to make a 100 bp double-stranded DNA fragment using Phusion polymerase. Then the gRNA cloning vector (http://www.addgene.org/41824/) was linearized using *Afl*II, and the 100 bp DNA fragment was incorporated into the above vector using Gibson assembly. N2a cells were cultured in six-well dishes to 70% confluence and co-transfected with Upf1 sgRNA plasmid plus Cas9 with Lipofectamine 2000. After a 48-h incubation, cells were selected by 500 µg/ml G418 with medium changes every 2 days until single colonies formed. After single colony isolation, stable cells were maintained with 200 µg/ml G418-containing medium for 1 week.

Transient transfection and RNAi

Transient transfections were performed by electroporation using a Microporator MP-100 (Digital Bio) or Neon-Transfection System (Invitrogen) and Lipofectamine 2000 (Invitrogen), according to the manufacturers' instructions. To knock down Upf1 expression, we selected sequences targeting coding sequence of *Upf1*. The knockdown-verified sense strand of *Upf1* shRNA is 5′-Tgatgcagttccgttccatc**TTCAAG**-AGAgatggaacggaactgcatc**TTTTTTC**-3′ (based on position 2185–2203 of mouse *Upf1*). The 19-nt *Upf1* target sequences are indicated in lower-case letters. The sense strand and antisense strand were annealed and cloned into the pLL3.7 lentiviral vector.

Dual luciferase reporter assay

For the reporter assay, N2a cells transfected with reporter or control plasmids were lysed in Reporter Lysis 5× Buffer (Promega, E3971). Renilla and firefly luciferase activities were determined using the Dual-Luciferase® Reporter Assay System (Promega), according to the manufacturer's instructions.

RNA-IP

N2a cells were lysed with RNA-IP buffer [10 mM HEPES (pH 7.5), 100 mM KCl, 5 mM $MgCl_2$, 0.1% NP-40, protease inhibitor]. Rat IgG or anti-Upf1 antibody was incubated with N2a cell lysates at 4°C overnight and then incubated with Protein G beads at 4°C for 4 h. We washed the beads three times with RNA-IP buffer and isolated RNA using TRI reagent. RNA levels were quantified by qRT-PCR.

RNA isolation and cDNA synthesis

RNA isolation and cDNA synthesis were performed as we previously described (Song et al., 2016). N2a cells were lysed with TRI-Solution (Bio Science Technology) and the total RNA was extracted after the addition of 0.2 volume of chloroform. Samples were mixed with vortex, incubated at room temperature for 10 min, and centrifuged at 12,000 ***g*** for 15 min at 4°C. Recovery of total RNA was performed by precipitation with 1/2 volume of isopropanol. After 10 min incubation at room temperature, samples were centrifuged at 12,000 ***g*** for 8 min at 4°C. The RNA pellet was washed with 75% ethanol, briefly air-dried and dissolved in diethylpyrocarbonate (DEPC)-treated water by incubating for 5 min at 65°C. The yield and purity of RNA were determined by a NanoDrop 2000 spectrophotometer (Thermo Fisher Scientific). Following quantification, 1µg of each total RNA sample was reverse transcribed using oligo-dT or random hexamer and the ImProm-II Reverse Transcription System (Promega), according to the manufacturer's instructions. For qRT-PCR analysis, each cDNA sample was diluted five times with nuclease-free water.

qRT-PCR

qRT-PCR was performed as we previously described (Song et al., 2016). The mRNA levels of endogenous genes or reporter plasmids were detected by qRT-PCR using a StepOnePlus Real-Time PCR System (Applied Biosystems) with FastStart Universal SYBR Green Master (Roche). A 20-µl sample of reaction cocktail was constituted of 3 µl diluted cDNA, 10 µl 2× SYBR Green Master Mix and 0.5 µl of each of the forward and reverse primers. The following amplification program was used: polymerase activation at 95°C for 10 min, 40 repeated cycles of 95°C for 15s and 60°C for 1 min. A comparative Ct method was used for quantification. The sequences of the forward and reverse primers are as follows: *Arc* (mRNA), 5′-TGAGACCAATTCCACTGATG-3′ and 5′-CTCCAGGGTCTCCCTA-GTCC-3′; *Arc* (mature-mRNA), 5′-CCCCCAGCAGTGATTCATAC-3′ and 5′-GTGATGCCCTTTCCAGACAT-3′; *Arc* (pre-mRNA), 5′-CTC-AGATCCCAGCCACTCTC-3′ and 5′-GTGATGCCCTTTCCAGACAT-3′; *Gapdh*, 5′-CATGGCCTTCCGTGTTCCTA-3′ and 5′-CCTGCTTCA-CCACCTTCTTGAT-3′; *Mef2a* (mRNA), 5′-ATCCGTTTACTGGGCTT-GTG-3′ and 5′-TGTCAGGACAGCAGATGAGG-3′; *Mef2a* (pre-mRNA), 5′-AGAAGGAAGAGTTGCGGTGA-3′ and 5′-ACACGCATAATGGA-TGAGAGG-3′; *Rpl32*, 5′-AACCCAGAGGCATTGACAAC-3′ and 5′-CACCTCCAGCTCCTTGACAT-3′; *Ago2*, 5′-AAGTCGGACAGGAGC-AGAAA-3′ and 5′-GAAACTTGCACTTCGCATCA-3′; *Dicer*, 5′-CTCG-TCAACTCTGCAAACCA-3′ and 5′-CAGTCAAGGCGACATAGCAA-3′; *Drosha*, 5′-AACAGTTCAACCCCGAAGTG-3′ and 5′-CTCTGAGCC-AGCTTCTGCTT-3′; β-actin, 5′-TATTGGCAACGAGCGG-3′ and 5′-CGGATGTCAACGTCAC-3′ and *Creb2*, 5′-CCTAGGTCTCTTAGATG-ACTATCTGGAGG-3′ and 5′-CCAGGTCATCCATTCGAAACAGAGC-ATCG-3′.

In vitro RNA synthesis and *in vitro* binding assay

For *in vitro* binding assays, biotin-UTP-labeled RNA was transcribed from the *Xba*I-linearized pSK-*Arc* 3′UTR plasmids or *Bam*HI-linearized psiCHECK2-*Arc* 3′UTR plasmids using T7 RNA polymerase (Promega, P2077). Streptavidin-biotin RNA affinity purification was performed as described previously (Seo et al., 2017). In brief, cell extracts prepared from N2a cells were incubated with biotinylated-*Arc* 3′UTR RNA and subjected to streptavidin resin adsorption. Resin-bound proteins were analyzed by SDS-PAGE.

Immunoblot analysis

N2a cells were lysed with RIPA buffer containing protease inhibitor tablet (Thermo Fisher Scientific, A32953), followed by sonication. Protein concentrations of lysates were determined using Bradford reagent (AMRESCO). Proteins were resolved by SDS-PAGE and transferred to nitrocellulose membranes (Pall Corporation), incubated with blocking buffer (5% non-fat dry milk in Tris-buffered saline and 0.1% Tween 20) for 30 min. Horseradish peroxidase-conjugated mouse (Thermo Fisher Scientific), rabbit (Promega), rat or goat (Bethyl Laboratories) secondary antibodies were detected with SUPEX ECL reagent (Neuronex) and an LAS-4000 system (Fujifilm), according to the manufacturers' instructions. Acquired images were analyzed using Image Gauge (Fujifilm) according to the manufacturer's instructions. The integrated blot density was quantified through ImageJ software-based analysis (http://rsb.info.nih.gov/ij/).

Antibodies

Antibodies used in this study included anti-Mef2a (1:500 dilution; Santa Cruz Biotechnology, sc-17785), anti-Ago2 (1:500 dilution; Santa Cruz Biotechnology, sc-376696), anti-GFP (1:1000 dilution; Santa Cruz Biotechnology, sc-8334), anti-CBP20 (1:100 dilution; Santa Cruz Biotechnology, sc-48793), anti-Cofilin (1:100 dilution; Abcam, ab54532), anti-p-Cofilin (1:1000 dilution; Santa Cruz Biotechnology, sc-12912), anti-14-3-3ζ (1:1000 dilution; Santa Cruz Biotechnology, sc-1019), anti-Arc (1:1000 dilution, SYSY, 156 003), anti-Gapdh (1:5000 dilution, Millipore, MAB374), anti-Flag (1:1000 dilution; Sigma-Aldrich, F1804), rabbit monoclonal anti-FLUC (1:10000 dilution, Abcam, ab185924) and mouse monoclonal anti-puromycin (1:1000 dilution, Merck, MABE343). Anti-Upf1 antibodies were generated and purified from rats immunized with carrier protein-conjugated peptide, DTQGSEFEFTDFTLPSQTQ or KDET-GELSSADEKRYRALK.

Polysome profiling

N2a cells were incubated in PBS containing 100 µg/ml CHX for 30 min on ice. The cells were lysed in polysome lysis buffer [300 mM KCl, 5 mM $MgCl_2$, 10 mM HEPES (pH 7.4), 0.5% NP-40, 5 mM DTT and 100 µg/ml CHX]. Cell lysates were loaded on 15–45% sucrose gradients in polysome buffer [300 mM KCl, 5 mM $MgCl_2$ and 10 mM HEPES (pH7.4)] and centrifuged at 32,000 rpm (175,117 ***g***) in a SW41Ti rotor at 4°C for 3 h. The gradients were collected using a Brandel gradient density fractionator and analyzed by an Econo UV monitor (Bio-Rad). Fractions (1 ml each) were spiked with 100 ng Renilla luciferase (Rluc) RNA to ensure the technical consistency of RNA isolation. RNAs were isolated from these fractions, and reverse transcription and qRT-PCR were performed.

Puro-PLA

N2a cells on chip glass were treated with 5 µM puromycin for 90 min at 37°C, 5% CO_2 and washed twice in PBS-MC (1× PBS, 1 mM $MgCl_2$, 0.1 mM $CaCl_2$). Cells were fixed in 4% paraformaldehyde (PFA; Sigma-Aldrich)-sucrose for 20 min and permeabilized with 0.5% Triton X-100 solution (Sigma-Aldrich) for 15 min. Duolink PLA reagents (Sigma-Aldrich) were used to detect newly synthesized proteins according to the manufacturer's instructions. The following antibodies were used for puro-PLA: rabbit monoclonal anti-FLUC (Abcam), anti-Arc (SYSY) and mouse monoclonal anti-puromycin (Merck). Nuclei of cells were stained with Hoechst 33342 and chip glasses were mounted with fluorescent mounting medium overnight. Duolink PLA signals were visualized by fluorescence microscopy (Olympus FV1000).

Immunocytochemistry and fluorescence microscopy

Transfected cells were maintained for 24 h, fixed with 4% PFA for 20 min. Nuclei of cells were stained with Hoechst 33342 and chip glasses were mounted with fluorescent mounting medium (Dako) overnight. The following antibodies were used for immunocytochemistry: rabbit monoclonal anti-FLUC (Abcam), anti-Upf1 (Sigma-Aldrich or Santa Cruz Biotechnology) and mouse monoclonal anti-puromycin (Merck). All images were obtained using a laser-scanning confocal microscope (model FV1000; Olympus) and IX71-Olympus inverted microscope with U-RFL-T (model IX71; Olympus), and FV10-ASW2.0 fluoviewer software was used for image analysis. We also used Alexa Fluor 568-conjugated phalloidin dye to label actin filaments.

Statistical analysis

All quantitative data are shown as mean±s.e.m. Statistical analyses were performed using Student's *t*-test, one-way analysis of variance (ANOVA) or two-way ANOVA and post-hoc Tukey's multiple comparison tests or Sidak's multiple comparisons using GraphPad software. *P*-values less than 0.05 were considered statistically significant. $*P<0.05$, $**P<0.01$, $***P<0.001$, $****P<0.0001$.

Acknowledgements

We are grateful to Dr Konstantin A. Lukyanov (Institute of Bioorganic Chemistry, Moscow, Russia) for providing dual-color fluorescent protein-based reporters for quantification of NMD activity, and to Dr Yoon Ki Kim (Korea University, Seoul, Korea) for providing the Flag_Upf1 plasmid.

Competing interests

The authors declare no competing or financial interests.

Author contributions

Conceptualization: H.G.R., J.-Y.S., Y.J., S.K.J., K.-T.K.; Methodology: H.G.R., J.-Y.S., Y.J., E.K.; Validation: H.G.R., K.-T.K.; Formal analysis: H.G.R., J.-Y.S., Y.J.; Investigation: H.G.R., J.-Y.S., S.W.K., E.K., S.K.J., K.-T.K.; Data curation: S.W.K.; Writing - original draft: H.G.R., J.-Y.S., Y.J., K.-T.K.; Writing - review & editing: H.G.R., J.-Y.S., Y.J., S.W.K., K.-T.K.; Visualization: H.G.R.; Supervision: H.G.R., K.-T.K.; Project administration: H.G.R., K.-T.K.; Funding acquisition: H.G.R., K.-T.K.

Funding

This work was supported by the Bio and Medical Technology Development program of the National Research Foundation of Korea [2018011982], the Cooperative Research Program for Agriculture Science and Technology Development of the Rural Development Administration [PJ01324801] and the BK21 Plus project of the Ministry of Education [10Z20130012243]. H.G.R. is supported by the KT&G Scholarship Foundation.

Supplementary information

Supplementary information available online at
http://jcs.biologists.org/lookup/doi/10.1242/jcs.224055.supplemental

References

Bamburg, J. R. and Bernstein, B. W. (2010). Roles of ADF/cofilin in actin polymerization and beyond. *F1000 Biol. Rep.* **2**, 62.

Belmonte, M. K., Allen, G., Beckel-Mitchener, A., Boulanger, L. M., Carper, R. A. and Webb, S. J. (2004). Autism and abnormal development of brain connectivity. *J. Neurosci.* **24**, 9228-9231.

Bliss, T. V. P. and Collingridge, G. L. (1993). A synaptic model of memory: long-term potentiation in the hippocampus. *Nature* **361**, 31-39.

Bramham, C. R. and Wells, D. G. (2007). Dendritic mRNA: transport, translation and function. *Nat. Rev. Neurosci.* **8**, 776-789.

Bramham, C. R., Worley, P. F., Moore, M. J. and Guzowski, J. F. (2008). The immediate early gene arc/arg3.1: regulation, mechanisms, and function. *J. Neurosci.* **28**, 11760-11767.

Bramham, C. R., Alme, M. N., Bittins, M., Kuipers, S. D., Nair, R. R., Pai, B., Panja, D., Schubert, M., Soule, J., Tiron, A. et al. (2010). The Arc of synaptic memory. *Exp. Brain Res.* **200**, 125-140.

Choe, J., Cho, H., Lee, H. C. and Kim, Y. K. (2010). microRNA/Argonaute 2 regulates nonsense-mediated messenger RNA decay. *EMBO Rep.* **11**, 380-386.

Choe, J., Cho, H., Chi, S.-G. and Kim, Y. K. (2011). Ago2/miRISC-mediated inhibition of CBP80/20-dependent translation and thereby abrogation of nonsense-mediated mRNA decay require the cap-associating activity of Ago2. *FEBS Lett.* **585**, 2682-2687.

Chowdhury, S., Shepherd, J. D., Okuno, H., Lyford, G., Petralia, R. S., Plath, N., Kuhl, D., Huganir, R. L. and Worley, P. F. (2006). Arc/Arg3.1 interacts with the endocytic machinery to regulate AMPA receptor trafficking. *Neuron* **52**, 445-459.

Farris, S., Lewandowski, G., Cox, C. D. and Steward, O. (2014). Selective localization of arc mRNA in dendrites involves activity- and translation-dependent mRNA degradation. *J. Neurosci.* **34**, 4481-4493.

Fiorini, F., Bagchi, D., Le Hir, H. and Croquette, V. (2015). Human Upf1 is a highly processive RNA helicase and translocase with RNP remodelling activities. *Nat. Commun.* **6**, 7581.

Flavell, S. W., Cowan, C. W., Kim, T. K., Greer, P. L., Lin, Y., Paradis, S., Griffith, E. C., Hu, L. S., Chen, C. and Greenberg, M. E. (2006). Activity-dependent regulation of MEF2 transcription factors suppresses excitatory synapse number. *Science* **311**, 1008-1012.

Gadjieva, R., Axelsson, E., Olsson, U., Vallon-Christersson, J. and Hansson, M. (2004). Nonsense-mediated mRNA decay in barley mutants allows the cloning of mutated genes by a microarray approach. *Plant Physiol. Biochem.* **42**, 681-685.

Giorgi, C., Yeo, G. W., Stone, M. E., Katz, D. B., Burge, C., Turrigiano, G. and Moore, M. J. (2007). The EJC factor eIF4AIII modulates synaptic strength and neuronal protein expression. *Cell* **130**, 179-191.

Hogg, J. R. and Goff, S. P. (2010). Upf1 senses 3′UTR length to potentiate mRNA decay. *Cell* **143**, 379-389.

Hurt, J. A., Robertson, A. D. and Burge, C. B. (2013). Global analyses of UPF1 binding and function reveal expanded scope of nonsense-mediated mRNA decay. *Genome Res.* **23**, 1636-1650.

Imamachi, N., Salam, K. A., Suzuki, Y. and Akimitsu, N. (2017). A GC-rich sequence feature in the 3′ UTR directs UPF1-dependent mRNA decay in mammalian cells. *Genome Res.* **27**, 407-418.

Isken, O., Kim, Y. K., Hosoda, N., Mayeur, G. L., Hershey, J. W. B. and Maquat, L. E. (2008). Upf1 phosphorylation triggers translational repression during nonsense-mediated mRNA decay. *Cell* **133**, 314-327.

Jankowsky, E. (2011). RNA helicases at work: binding and rearranging. *Trends Biochem. Sci.* **36**, 19-29.

Kawashima, T., Okuno, H., Nonaka, M., Adachi-Morishima, A., Kyo, N., Okamura, M., Takemoto-Kimura, S., Worley, P. F. and Bito, H. (2009). Synaptic activity-responsive element in the Arc/Arg3.1 promoter essential for synapse-to-nucleus signaling in activated neurons. *Proc. Natl. Acad. Sci. USA* **106**, 316-321.

Kawashima, T., Kitamura, K., Suzuki, K., Nonaka, M., Kamijo, S., Takemoto-Kimura, S., Kano, M., Okuno, H., Ohki, K. and Bito, H. (2013). Functional labeling of neurons and their projections using the synthetic activity-dependent promoter E-SARE. *Nat. Methods* **10**, 889-895.

Kim, D.-Y., Kwak, E., Kim, S.-H., Lee, K.-H., Woo, K.-C. and Kim, K.-T. (2011). hnRNP Q mediates a phase-dependent translation-coupled mRNA decay of mouse Period3. *Nucleic Acids Res.* **39**, 8901-8914.

Klann, E. and Dever, T. E. (2004). Biochemical mechanisms for translational regulation in synaptic plasticity. *Nat. Rev. Neurosci.* **5**, 931-942.

Lanahan, A. and Worley, P. (1998). Immediate-early genes and synaptic function. *Neurobiol. Learn. Mem.* **70**, 37-43.

Lee, K.-H., Kim, S.-H., Kim, H.-J., Kim, W., Lee, H.-R., Jung, Y., Choi, J.-H., Hong, K. Y., Jang, S. K. and Kim, K.-T. (2014). AUF1 contributes to Cryptochrome1 mRNA degradation and rhythmic translation. *Nucleic Acids Res.* **42**, 3590-3606.

Lee, E., Ryu, H. G., Kim, S., Lee, D., Jeong, Y.-H. and Kim, K.-T. (2016). Glycogen synthase kinase 3beta suppresses polyglutamine aggregation by inhibiting Vaccinia-related kinase 2 activity. *Sci. Rep.* **6**, 29097.

Mali, P., Yang, L., Esvelt, K. M., Aach, J., Guell, M., DiCarlo, J. E., Norville, J. E. and Church, G. M. (2013). RNA-guided human genome engineering via Cas9. *Science* **339**, 823-826.

McKinsey, T. A., Zhang, C. L. and Olson, E. N. (2002). MEF2: a calcium-dependent regulator of cell division, differentiation and death. *Trends Biochem. Sci.* **27**, 40-47.

Mendell, J. T., Sharifi, N. A., Meyers, J. L., Martinez-Murillo, F. and Dietz, H. C. (2004). Nonsense surveillance regulates expression of diverse classes of mammalian transcripts and mutes genomic noise. *Nat. Genet.* **36**, 1073-1078.

Messaoudi, E., Kanhema, T., Soule, J., Tiron, A., Dagyte, G., da Silva, B. and Bramham, C. R. (2007). Sustained Arc/Arg3.1 synthesis controls long-term potentiation consolidation through regulation of local actin polymerization in the dentate gyrus in vivo. *J. Neurosci.* **27**, 10445-10455.

Ninomiya, K., Ohno, M. and Kataoka, N. (2016). Dendritic transport element of human arc mRNA confers RNA degradation activity in a translation-dependent manner. *Genes Cells* **21**, 1263-1269.

Pai, B., Siripornmongcolchai, T., Berentsen, B., Pakzad, A., Vieuille, C., Pallesen, S., Pajak, M., Simpson, T. I., Armstrong, J. D., Wibrand, K. et al. (2014). NMDA receptor-dependent regulation of miRNA expression and association with Argonaute during LTP in vivo. *Front. Cell Neurosci.* **7**, 285.

Pan, Q., Saltzman, A. L., Kim, Y. K., Misquitta, C., Shai, O., Maquat, L. E., Frey, B. J. and Blencowe, B. J. (2006). Quantitative microarray profiling provides evidence against widespread coupling of alternative splicing with nonsense-mediated mRNA decay to control gene expression. *Genes Dev.* **20**, 153-158.

Panja, D., Kenney, J. W., D'Andrea, L., Zalfa, F., Vedeler, A., Wibrand, K., Fukunaga, R., Bagni, C., Proud, C. G. and Bramham, C. R. (2014). Two-stage translational control of dentate gyrus LTP consolidation is mediated by sustained BDNF-TrkB signaling to MNK. *Cell Rep* **9**, 1430-1445.

Paolantoni, C., Ricciardi, S., De Paolis, V., Okenwa, C., Catalanotto, C., Ciotti, M. T., Cattaneo, A., Cogoni, C. and Giorgi, C. (2018). Arc 3′ UTR splicing leads to dual and antagonistic effects in fine-tuning arc expression upon BDNF signaling. *Front. Mol. Neurosci.* **11**, 145.

Park, S., Park, J. M., Kim, S., Kim, J.-A., Shepherd, J. D., Smith-Hicks, C. L., Chowdhury, S., Kaufmann, W., Kuhl, D., Ryazanov, A. G. et al. (2008). Elongation factor 2 and fragile X mental retardation protein control the dynamic translation of Arc/Arg3.1 essential for mGluR-LTD. *Neuron* **59**, 70-83.

Pereverzev, A. P., Gurskaya, N. G., Ermakova, G. V., Kudryavtseva, E. I., Markina, N. M., Kotlobay, A. A., Lukyanov, S. A., Zaraisky, A. G. and Lukyanov, K. A. (2015). Method for quantitative analysis of nonsense-mediated mRNA decay at the single cell level. *Sci. Rep.* **5**, 7729.

Pesole, G., Liuni, S., Grillo, G., Licciulli, F., Larizza, A., Makalowski, W. and Saccone, C. (2000). UTRdb and UTRsite: specialized databases of sequences and functional elements of 5′ and 3′ untranslated regions of eukaryotic mRNAs. *Nucleic Acids Res.* **28**, 193-196.

Plath, N., Ohana, O., Dammermann, B., Errington, M. L., Schmitz, D., Gross, C., Mao, X., Engelsberg, A., Mahlke, C., Welzl, H. et al. (2006). Arc/Arg3.1 is essential for the consolidation of synaptic plasticity and memories. *Neuron* **52**, 437-444.

Rose, A. B. (2004). The effect of intron location on intron-mediated enhancement of gene expression in Arabidopsis. *Plant J.* **40**, 744-751.

Sanchez, G., Bondy-Chorney, E., Laframboise, J., Paris, G., Didillon, A., Jasmin, B. J. and Côté, J. (2016). A novel role for CARM1 in promoting nonsense-mediated mRNA decay: potential implications for spinal muscular atrophy. *Nucleic Acids Res.* **44**, 2661-2676.

Seo, J. Y., Kim, D. Y., Kim, S. H., Kim, H. J., Ryu, H. G., Lee, J., Lee, K. H. and Kim, K. T. (2017). Heterogeneous nuclear ribonucleoprotein (hnRNP) L promotes DNA damage-induced cell apoptosis by enhancing the translation of p53. *Oncotarget* **8**, 51108-51122.

Song, H., Kim, W., Kim, S.-H. and Kim, K.-T. (2016). VRK3-mediated nuclear localization of HSP70 prevents glutamate excitotoxicity-induced apoptosis and Abeta accumulation via enhancement of ERK phosphatase VHR activity. *Sci. Rep.* **6**, 38452.

Steward, O., Wallace, C. S., Lyford, G. L. and Worley, P. F. (1998). Synaptic activation causes the mRNA for the IEG Arc to localize selectively near activated postsynaptic sites on dendrites. *Neuron* **21**, 741-751.

Sutton, M. A. and Schuman, E. M. (2006). Dendritic protein synthesis, synaptic plasticity, and memory. *Cell* **127**, 49-58.

Tani, H., Imamachi, N., Salam, K. A., Mizutani, R., Ijiri, K., Irie, T., Yada, T., Suzuki, Y. and Akimitsu, N. (2012). Identification of hundreds of novel UPF1 target transcripts by direct determination of whole transcriptome stability. *RNA Biol.* **9**, 1370-1379.

Toma, K. G., Rebbapragada, I., Durand, S. and Lykke-Andersen, J. (2015). Identification of elements in human long 3′ UTRs that inhibit nonsense-mediated decay. *RNA* **21**, 887-897.

Viegas, M. H., Gehring, N. H., Breit, S., Hentze, M. W. and Kulozik, A. E. (2007). The abundance of RNPS1, a protein component of the exon junction complex, can determine the variability in efficiency of the Nonsense Mediated Decay pathway. *Nucleic Acids Res.* **35**, 4542-4551.

Waltereit, R., Dammermann, B., Wulff, P., Scafidi, J., Staubli, U., Kauselmann, G., Bundman, M. and Kuhl, D. (2001). Arg3.1/Arc mRNA induction by Ca2+ and cAMP requires protein kinase A and mitogen-activated protein kinase/extracellular regulated kinase activation. *J. Neurosci.* **21**, 5484-5493.

Waung, M. W., Pfeiffer, B. E., Nosyreva, E. D., Ronesi, J. A. and Huber, K. M. (2008). Rapid translation of Arc/Arg3.1 selectively mediates mGluR-dependent LTD through persistent increases in AMPAR endocytosis rate. *Neuron* **59**, 84-97.

Wibrand, K., Pai, B., Siripornmongcolchai, T., Bittins, M., Berentsen, B., Ofte, M. L., Weigel, A., Skaftnesmo, K. O. and Bramham, C. R. (2012). MicroRNA regulation of the synaptic plasticity-related gene Arc. *PLoS ONE* **7**, e41688.

Yepiskoposyan, H., Aeschimann, F., Nilsson, D., Okoniewski, M. and Muhlemann, O. (2011). Autoregulation of the nonsense-mediated mRNA decay pathway in human cells. *RNA* **17**, 2108-2118.